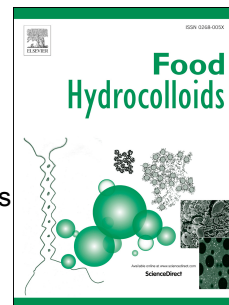


Journal Pre-proof

Effect of concentrations of alginate, soy protein isolate and sunflower oil on water loss, shrinkage, elastic and structural properties of alginate-based emulsion gel beads during gelation

Duanquan Lin, Alan L. Kelly, Valentyn Maidannyk, Song Miao



PII: S0268-005X(20)30100-4

DOI: <https://doi.org/10.1016/j.foodhyd.2020.105998>

Reference: FOOHYD 105998

To appear in: *Food Hydrocolloids*

Received Date: 15 January 2020

Revised Date: 25 April 2020

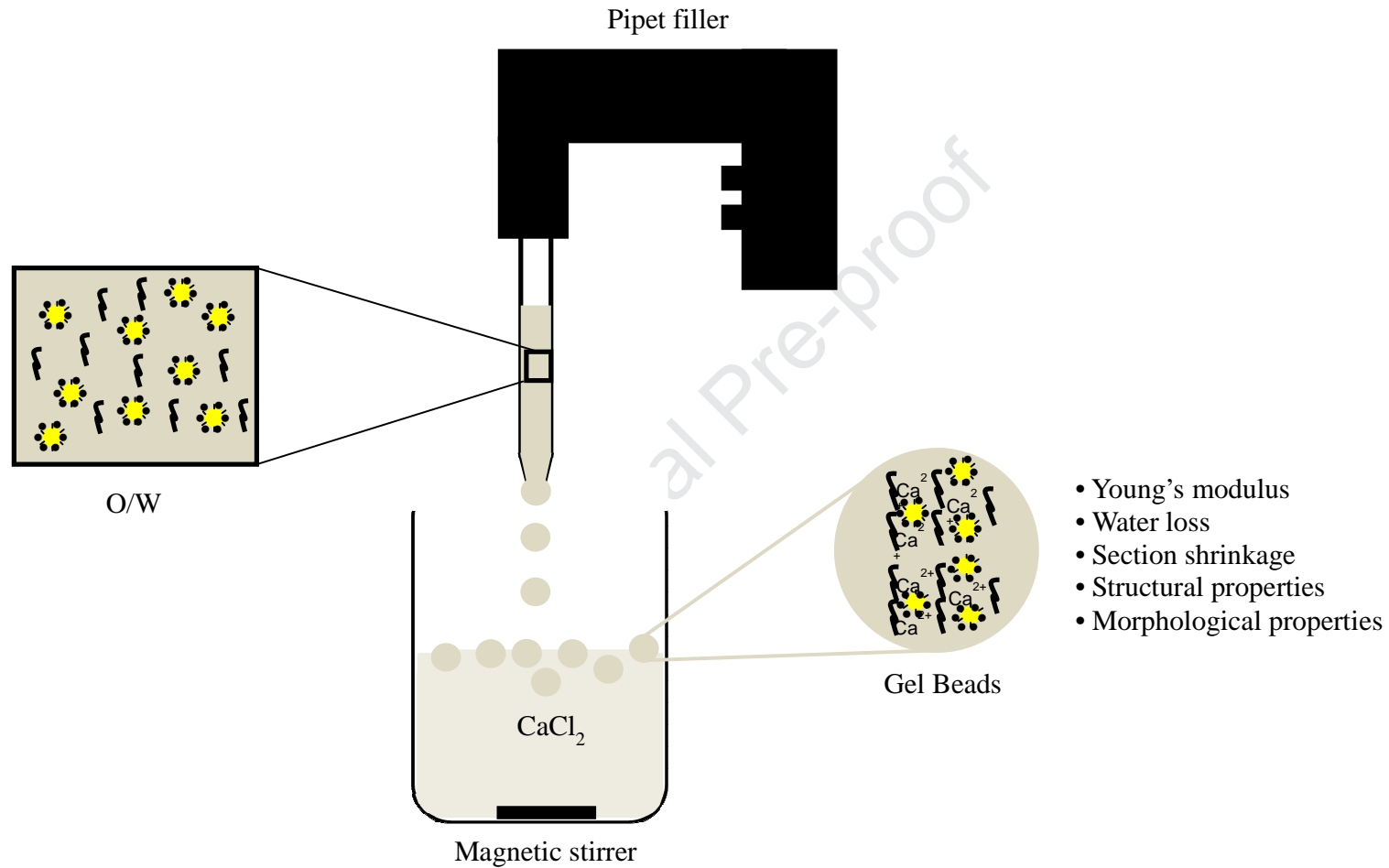
Accepted Date: 4 May 2020

Please cite this article as: Lin, D., Kelly, A.L., Maidannyk, V., Miao, S., Effect of concentrations of alginate, soy protein isolate and sunflower oil on water loss, shrinkage, elastic and structural properties of alginate-based emulsion gel beads during gelation, *Food Hydrocolloids* (2020), doi: <https://doi.org/10.1016/j.foodhyd.2020.105998>.


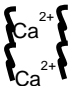
This is a PDF file of an article that has undergone enhancements after acceptance, such as the addition of a cover page and metadata, and formatting for readability, but it is not yet the definitive version of record. This version will undergo additional copyediting, typesetting and review before it is published in its final form, but we are providing this version to give early visibility of the article. Please note that, during the production process, errors may be discovered which could affect the content, and all legal disclaimers that apply to the journal pertain.

© 2020 Published by Elsevier Ltd.

Graphical Abstracts



- SPI
- ⌋ Sodium alginate

-  O/W droplet structure
-  Alginate gel structure

1 **Effect of concentrations of alginate, soy protein isolate and sunflower oil on water loss,**
2 **shrinkage, elastic and structural properties of alginate-based emulsion gel beads during**
3 **gelation**

4 Duanquan Lin^{1,2}, Alan L. Kelly², Valentyn Maidannyk¹, Song Miao^{1,2,3*}

5 ¹*Teagasc Food Research Centre, Moorepark, Fermoy, Co. Cork, Ireland*

6 ²*School of Food and Nutritional Sciences, University College Cork, Cork, Ireland*

7 ³*China-Ireland International Cooperation Centre for Food Material Science and Structure*
8 *Design, Fuzhou, China*

9
10 *Corresponding author

11 Dr. Song Miao

12 Tel: +353 2542468

13 Fax: +353 2542340

14 E-mail: song.miao@teagasc.ie

15 **Abstract**

16 The aim of this study was to investigate the influence of concentrations of sodium alginate
17 (0.5%–1.5% in the water phase of an emulsion), soy protein isolate (SPI, 0.5%–2.0% in the
18 water phase) and oil phase (10%–40% in the emulsion) on the properties (including water
19 loss, shrinkage, morphological, elastic, and structural properties) of emulsion gel beads
20 during gelation (0–30 min). Gel beads were prepared with external gelation by dropping
21 emulsions into CaCl_2 solutions using pipettes. The Young's modulus of emulsion gel beads
22 kept increasing during gelation before reaching a plateau accompanied by syneresis (i.e.,
23 water loss), shrinkage, and structural tightening. SPI absorbed at the surface of oil droplets
24 could prevent re-coalescence of droplets during gelation. Additionally, increasing
25 concentrations of sodium alginate and oil increased the Young's modulus of gel beads. Water
26 loss decreased with increasing contents of alginate, SPI and oil, and shrinkage could be
27 diminished by increasing alginate and oil contents.

28 **Keywords:** Alginate; Elastic property; Emulsion gel bead; Microstructure; Shrinkage; Soy
29 protein isolates.

30 **1. Introduction**

31 Emulsion gels, also called emulgels, are a complex colloidal material which have some
32 properties of both emulsions and gels (Dickinson, 2012). During the last decade, emulsion
33 gels have received growing interest, due to their advantages compared to emulsions, such as
34 higher storage stability by reducing oil and water phase movement and lipid oxidation (Ma,
35 Wan, & Yang, 2017) and slower intestinal drug release, due to improved protective effects
36 against gastric and intestinal phases (Corstens, Berton-Carabin, Elichiry-Ortiz, Hol, Troost,
37 Masclee, et al., 2017; Guo, Bellissimo, & Rousseau, 2017). In order to produce emulsion
38 gels, emulsions are first prepared by mixing gelling agent, emulsifier and oil and then turned
39 into gels by different gelation mechanisms.

40 The choice of matrix material and emulsifier is the key factor in structuring emulsion gels.
41 Proteins (e.g., soy protein isolate (SPI) and whey protein isolate (WPI)) and polysaccharides
42 (e.g., agar and gellan gum) have been widely investigated as gelling agents in the formation
43 of emulsion gels (Brito-Oliveira, Bispo, Moraes, Campanella, & Pinho, 2017; Geremias-
44 Andrade, Souki, Moraes, & Pinho, 2017; Guo, et al., 2017). Different gelling agents can form
45 different gelation structures, and the gelation mechanism (e.g., heat, high pressure,
46 acidification, enzymatic treatment, and addition of ions) for different gelling agents differs
47 (Dickinson, 2012), which can affect the properties of emulsion gels and encapsulated food
48 nutrients. Both synthetic (e.g., Tween 80 and Span 80) and natural (e.g., proteins, egg
49 lecithin, and soy lecithin) emulsifiers can be used to prepare emulsion gels. Lipid droplets in
50 emulsion gels can be divided into active and inactive fillers according to the interactions
51 between gelling agents and emulsifier-coated lipid droplets (Van Vliet, 1988; Yang et al.,
52 2020), which can also influence the properties of emulsion gels (Geremias-Andrade, et al.,
53 2017).

54 Alginate, a linear unbranched natural polysaccharide, is derived from brown seaweed extracts
55 (*Phaeophyceae*) (King, 1983) and composed of two monomeric isomers: β -(1 \rightarrow 4)-linked D-
56 mannuronic acid (M) residues and α -(1 \rightarrow 4)-linked L-guluronic acid (G) residues (Ching,
57 Bansal, & Bhandari, 2017). Alginate-based emulsion gels received high attention in recent
58 years (Lević, Pajić Lijaković, Đorđević, Rac, Rakić, Šolević Knudsen, et al., 2015; Qu, Zhao,
59 Fang, Nishinari, Phillips, Wu, et al., 2016; Zeeb, Saberi, Weiss, & McClements, 2015).

60 Alginate monomers can form gels by ionic crosslinking with divalent cations (mostly calcium
61 cations in the food industry) (King, 1983). External gelation and internal gelation are two
62 methods used to prepare alginate-based emulsion gels. Pintado, Ruiz-Capillas, Jimenez-
63 Colmenero, Carmona, & Herrero (2015) added CaSO₄ into an alginate-based emulsion to
64 directly produce an alginate-based emulsion gel. Sato, Moraes, & Cunha (2014) used internal
65 method to produce emulsion gels, in which CaEDTA was added to an alginate-based
66 emulsion first, after which acid was introduced to liberate calcium ions. Compared these two
67 methods, Puguang, Yu, and Kim (2014) found that gels formed by external gelation had a
68 smoother surface and denser inner structure. In addition, alginate-based gels are not sensitive
69 to gastric fluids, and can protect the encapsulated nutrients from harsh gastric environment,
70 and the remaining gel structures can be further disrupted during intestinal digestion
71 accompanied by the release of encapsulated compounds (Zhang, et al., 2016).

72 Previous studies mainly focused on the formulation, structural properties, mechanical
73 properties, stability, and digestion of alginate-based emulsion gels. However, there are few
74 reports on the gelation process of alginate-based emulsion gels. It has been indicated that,
75 during the gelation process of alginate hydrogels prepared by external gelation, calcium
76 cations can diffuse into alginate drops after being dropped into a calcium chloride solution
77 (Rehm, 2009). Syneresis also occurs during this gelation process, with a consequent decrease
78 in dimensions of gel beads (Quong, Neufeld, Skjåk-Bræk, & Poncelet, 1998; Rehm, 2009).

79 However, the gelation process of alginate-based emulsion gels may differ from that of
80 alginate gels, because the presence of lipids and emulsifiers in emulsions may affect the
81 gelation process. Understanding the gelation process of alginate-based emulsion gels may
82 help to produce emulsion gels with specific properties (e.g., size, water content, mechanical
83 properties) by controlling gelation time, formulation, preparation methods and processing
84 technologies. Therefore, further studies are needed to understand how alginate, emulsifiers
85 and oil affect the gelation process of emulsion gel beads.

86 The purpose of this study was thus to investigate the gelation process of alginate-based
87 emulsion gel beads. In order to improve the encapsulation efficiency and hygroscopicity of
88 alginate-based emulsion gels, proteins (e.g., lupin protein and WPI) can be used as
89 emulsifiers (Corstens, et al., 2017; Piornos, Burgos-Díaz, Morales, Rubilar, & Acevedo,
90 2017), and polysaccharides (e.g., *Prosopis alba* exudate gum and chitosan) can be used as
91 structural strengthening agents (Natrajan, Srinivasan, Sundar, & Ravindran, 2015; Vasile,
92 Judis, & Mazzobre, 2018). In this study, denatured SPI was thus introduced as surfactant,
93 because SPI has a huge potential value in producing emulsion gels, due to its good
94 emulsifying property, and denatured SPI has increased emulsifying capacity compared to
95 natural SPI (Lin, Lu, Kelly, Zhang, Zheng, & Miao, 2017; Nishinari, Fang, Guo, & Phillips,
96 2014). In addition, the external gelation was used, in order to obtain gel beads with denser
97 structures, compared to internal gelation. Effect of concentrations of alginate, SPI, and
98 sunflower oil on the shrinkage, water loss, elastic and structural properties of alginate-based
99 emulsion gel beads during gelation were investigated in this study.

100 **2. Materials and methods**

101 *2.1. Materials*

102 Defatted soy flour (Bob's Red Mill, Milwaukie, Oregon, USA) and sunflower oil (Aldi Stores
103 Ltd., Kildare, Ireland) were purchased from iHerb and Aldi, respectively. Sodium alginate
104 was obtained from Special Ingredients (Chesterfield, UK). Calcium chloride, sodium
105 hydroxide, and hydrochloric acid were purchased from Sigma-Aldrich (St. Louis, MO, USA).

106 *2.2. Preparation of soy protein isolate*

107 SPI was prepared according to the method described by Urbonaite, Jongh, Linden and
108 Pouvreau (2015). The defatted soy flour was suspended in distilled water at a ratio of 1:10
109 (w/w) at 45 °C and stirred for 30 min. The pH value was then adjusted to 8.0 with 5 M
110 NaOH, and the solution was stirred for 30 min in the water bath. The supernatant was
111 collected by centrifugation (30 min, 6000×g, 13 °C) (Sorvall LYNX 6000 Superspeed
112 Centrifuge, Thermo Fisher Scientific, Waltham, USA). Protein isolates were obtained by
113 isoelectric precipitation by adjusting the pH value to 4.5 with 6 M HCl. After mild stirring for
114 12 h at 5 °C, the suspension was centrifuged (30 min, 6000×g, 7 °C). The sediment was re-
115 suspended three times in deionized water at a ratio of 1:3 (w/w) and filtered by multilayer
116 gauze to remove any remaining insoluble material, and the filtrate was centrifuged (30 min,
117 6000×g, 7 °C) again. The sediment was finally suspended in deionized water at a ratio of 1:4
118 (w/w), and the pH value was justified to 7.0 with 5 M NaOH. Then, the solution was freeze-
119 dried (Free Zone 12 Freeze Dry System, Labconco Corporation, Kansas, MO, USA). The
120 dried SPI was kept in polyethylene bags and stored at room temperature. The protein content
121 of SPI powder was $96.29 \pm 0.03\%$.

122 *2.3. Preparation of alginate-based and SPI-stabilized emulsions and gel beads*

123 A dispersion of soy protein isolate (5% wt in distilled water) was stirred at room temperature
124 for 30 min using a magnetic stirrer, heated at 90 °C for 30 min, and then cooled to room
125 temperature. For the production of continuous phase, sodium alginate (0.5, 1.0, and 1.5% wt)

126 was added into the pre-heated soy protein isolate solution with adding water to reach final
127 concentrations of SPI (0.5, 1.0, and 2.0% wt) by shearing at 400 rpm for 30 min with a
128 magnetic stirrer and then allowed to rest for 24 h to permit hydration. For the production of
129 o/w emulsion, sunflower oil (10, 20, and 40% wt) was added to above continuous phase and
130 mixed at 18,000 rpm for 2 min with an Ultra-Turrax (IKA-25, Staufen, Germany). Solutions
131 containing 1.0% alginate (1A) and dispersions containing 1.0% alginate and 1.0% SPI
132 (1A1S) were prepared as control groups without mixing at 18,000 rpm for 2 min. Table 1
133 shows the formulations used for preparing emulsions.

134 For producing gel beads, the resulting dispersions/solutions were dropped into 2 % (w/w)
135 $\text{CaCl}_2 \cdot 2\text{H}_2\text{O}$ solutions using 5-ml measuring pipettes and a S1 pipette filler (Thermo Fisher
136 Scientific Inc., Waltham, USA). The distance between the tip of pipette and the surface of
137 CaCl_2 solutions was fixed at 10 cm. The samples were allowed to gel in CaCl_2 solutions for
138 30 min with mild magnetic stirring, and the resulting beads were rinsed with distilled water.
139 Samples were analyzed immediately for measurement of Young's modulus, shrinkage, water
140 loss, and morphology, and samples were kept in distilled water for observing their structures
141 within 3 hours after being prepared.

142 *2.4. Properties of dispersions/solutions*

143 *2.4.1. Structures*

144 Confocal scanning laser microscopy (CLSM) was used to observe microstructures of
145 dispersions/emulsions. Dispersion/emulsion samples (500 μl) were transferred to a glass slide
146 and stained with 50 μl of a mixture of Nile red (0.1%, w/v, in polyethylene glycol-200) and
147 fast green (0.1%, w/v, in distilled water) at a ratio of 3:1. Confocal observation was
148 performed using a Leica TCS SP5 microscope (Leica Microsystems GmbH, Wetzlar,

149 Germany) at excitation and emission wavelengths of 488 nm and 633 nm, provided by an
150 argon laser and a HeNe laser, respectively.

151 2.4.2. Viscosity

152 The viscosity of dispersions/solutions was tested at 25 °C using an AR 2000ex rheometer (TA
153 Instruments, Crawley, UK) with an aluminium parallel plate (60 mm in diameter, and 0.5 mm
154 in gap). Each sample was added in the middle of Peltier plate and allowed to stand for 2 min
155 before testing. The flow measurement was performed over a shear rate range of 0.1 to 100 s⁻¹,
156 and viscosity (η) was obtained from the data analysis software.

157 2.5. Microstructures of gel beads

158 CLSM was used to observe microstructures of gel beads. Each gel bead was cut into a thin
159 layer (~ 1 mm), transferred to a glass slide, and stained with a mixture of Nile red (0.1%, w/v,
160 in polyethylene glycol-200) and fast green (0.1%, w/v, in distilled water) at a ratio of 3:1.
161 Confocal observation was performed by the method described in section 2.4.1.

162 2.6. Young's modulus of gel beads

163 The Young's modulus of gel beads during gelation at 1, 2, 3, 4, 5, 6, 8, 10, 20, and 30 min
164 were analysed by a TA.XT Plus texture analyser (Stable Micro System, Godalming, UK)
165 according the method described by Ching, Bansal, & Bhandari (2016) with a minor change.
166 The surface of samples was dried with dry paper before testing. Compression tests were
167 performed using a cylinder probe of 10-mm diameter and a 5-kg load cell. The samples were
168 compressed to 30% strain at a crosshead speed of 0.1 mm/s, and five beads with same
169 composition were examined one after another. Due to their ellipsoidal shapes, the cross-
170 sectional area of samples was calculated after measuring the major axis and minor axis of
171 samples after being placed on the platform of texture analyser. The Young's modulus of each

172 sample was calculated as the gradient of the stress vs. strain curve in the 5–15% strain region,
 173 where stress and strain showed good linearity. The experiment was performed in triplicate.

174 2.7. Water loss of gel beads

175 The water loss of samples during gelation was determined at 1, 2, 3, 4, 5, 6, 8, 10, 20, and 30
 176 min after dispersions/solutions were dropped into calcium chloride solutions. In this study,
 177 the water loss means the decreased water in gel beads during gelation compared to the
 178 original dispersions/solutions. Five gel particles were obtained from calcium chloride
 179 solutions and washed with distilled water. After drying the surface, the initial weight of 5
 180 beads was weighted (W'_i) and then they were dried in an oven at 80 °C until constant weight
 181 (W'_d). The initial weight (W_i) and the weight after drying (W_d) of dispersions/solutions (5
 182 drops) were determined by the same method. Thus, the water loss was calculated from Eq.
 183 (1), if we assumed that the main content (i.e., alginate, SPI, and oil) of gel beads have no
 184 significant change during gelation, and the experiment was replicated three times.

$$185 \text{ Water loss (\%)} = \left(\frac{W_i - W_d}{W_i} - \frac{W_d}{W_i} \times \frac{W'_i - W'_d}{W'_d} \right) \times 100\% \quad (1)$$

186 2.8. Shrinkage of gel beads

187 The section shrinkage rate of gel beads was determined at 2, 4, 6, 8, 10, 20, and 30 min after
 188 dispersions/solutions were dropped into calcium chloride solutions. Five gel beads were
 189 obtained from the calcium chloride solutions and washed with distilled water. After drying
 190 the surface, photographs of gel beads were taken using a camera (iPhone 7 plus, Apple Inc.,
 191 California, USA). The major semi-axis (r'_{\max}) and minor semi-axis (r'_{\min}) of gel beads were
 192 measured by using a digital vernier calliper, and the section area (A'_s) was calculated from
 193 Eq. (2). The major semi-axis (r_{\max}) and minor semi-axis (r_{\min}) of gel beads after gelation for 1
 194 min were measured, and the section area (A_s) was also calculated from Eq. (2). The section

195 shrinkage rate of gel beads was calculated from Eq. (2), and the experiment was replicated
 196 three times. It should be noted that the section shrinkage rate of samples during gelation
 197 process was compared to the section area of samples after gelation for 1 min in this study.

$$198 \text{ Section shrinkage rate (\%)} = \frac{A_s - A'_s}{A_s} = \frac{3.14 \times r_{max} \times r_{min} - 3.14 \times r'_{max} \times r'_{min}}{3.14 \times r_{max} \times r_{min}} \times 100\% \quad (2)$$

199 3. Results and discussion

200 3.1 Structural properties of gel beads

201 Structural properties are important for emulsion gels because they can influence mechanical
 202 properties of emulsion gels and release behavior of encapsulated nutrients. Many factors
 203 (e.g., structures of the gel matrix, structures of emulsion droplets, and interactions between
 204 the gel matrix and droplets) can influence the structures of overall emulsion gels. Therefore,
 205 the effect of concentrations of alginate, SPI and oil on the structures of emulsions and
 206 emulsion gels was investigated in this study.

207 Fig. 1 shows the structures of emulsions/dispersions before gelation and gel beads after
 208 gelation for 30 min. In sample 1A1S, SPI formed aggregates and dispersed in alginate
 209 solutions (Figs. 1A and 1V). This was because SPI was heated at 90°C for 30 min in this
 210 study, and thus the solubility of SPI decreased, due to denaturation; additionally, denatured
 211 SPI exposed hydrophobic residues and thus formed aggregations in alginate solutions
 212 (Wagner & Añón, 1990). After mixing the 1A1S dispersion with oil, SPI modules can move
 213 from the continuous phase to the O/W interfaces and are absorbed at the surface of oil
 214 droplets (Figs. 1A and 1B), due to their amphipathic nature and emulsifying capacity.
 215 Hydrophobic groups of SPI absorbed onto the surface of oil droplets, and hydrophilic groups
 216 connected with the water phase, acting as a steric barrier against coalescence of oil droplets
 217 (Nishinari, et al., 2014). However, increasing the alginate concentration to 1.5% led to more

218 SPI aggregations in the water phase (Figs. 1B and 1C), because the higher viscosity of the
219 continuous phase of emulsions hindered SPI from moving to the oil–water interface
220 (Tavernier, Patel, Van der Meeren, & Dewettinck, 2017). Higher SPI concentrations resulted
221 in more SPI being absorbed at the surface of oil droplets but led to more obvious flocculation
222 of oil droplets (Figs. 1B and 1D), probably due to the depletion flocculation of droplets
223 coated by excessive amount of SPI (Moschakis, Murray, & Biliaderis, 2010). In addition,
224 increasing oil content of emulsions resulted in more compacted gel structures (Figs. 1B and
225 1E), due to the decreased ratio of the water phase to the oil phase.

226 Fig. 1 also indicates that there were more dark sections in emulsions/dispersions than gel
227 beads in all samples, which indicates that syneresis and shrinkage of the water phase during
228 gelation led to more compact filler structures. In addition, the concentrations of SPI, alginate
229 and oil could affect the stability of droplets during gelation. As shown in Figs. 1B and 1W
230 SPI-coated droplets in sample 1A1S20O could maintain their structures during gelation. This
231 was because SPI could stabilize the o/w emulsions, and gelation, syneresis and shrinkage
232 mainly occurred in the water phase during gelation, which had no significant effects on the
233 structures of emulsion droplets. Similarly, it was found that WPI-aggregate-stabilized
234 emulsions were stable during the gelation period (Rosa, Sala, Van Vliet, & Van De Velde,
235 2006). Additionally, higher SPI concentration resulted in more stable droplet structures
236 during gelation, probably because of more SPI being absorbed at the surface of oil droplets
237 (Figs. 1D and 1Y). However, increasing the alginate concentration to 1.5% led to re-
238 coalescence of droplets during gelation (Figs. 1C and 1X), because increased viscosity of the
239 continuous phase of emulsions hindered SPI from moving to the oil–water interface and thus
240 resulted in decreased stability of emulsion droplets during gelation. In addition, increasing the
241 oil content to 40% also led to re-coalescence of droplets during gelation (Figs. 1E and 1Z),
242 probably because 1.0% SPI in the water phase was not enough to stabilize 40% oil.

243 3.2. Young's modulus of gel beads

244 3.2.1. The profiles of Young's modulus during gelation

245 Compression tests were carried out to study the elastic properties of gel beads during
246 gelation. Firstly, the effect of introducing SPI and oil into alginate gels on the profiles of
247 Young's modulus during gelation was investigated. As shown in Fig. 2A, the changes of
248 Young's modulus of gel beads containing 1% alginate (1A in short) included three steps:
249 increasing up to 5 min, decreasing between 5 and 10 min, and then reaching a plateau. The
250 Young's modulus of gel beads containing 1% alginate and 1% SPI (sample 1A1S) had a
251 similar trend to that of sample 1A, but the Young's modulus of emulsion gel beads containing
252 1% alginate, 1% SPI, and 20% oil (sample 1A1S20O) increased first and then reached a
253 plateau at 8 min directly (Fig. 2A). It can be seen that the gelation process of alginate-based
254 gel beads includes the maturation step (increased Young's modulus), the structural collapse
255 step (decreased Young's modulus), and the equilibrium step (unchanged Young's modulus).
256 Therefore, it was assumed that the gelation mechanism of alginate beads prepared by the
257 external gelation has a direct effect on the changes in Young's modulus during gelation.

258 After being dropped into calcium chloride solutions, the surface of alginate drops can gel
259 instantaneously, and then Ca^{2+} can diffuse from the CaCl_2 solutions into the interior of
260 alginate drops, which leads to the gelation of gel beads from outside to inside and increased
261 Young's modulus (Ching, et al., 2017). This process is called the maturation step (Puguan, et
262 al., 2014). The concentration of alginate solutions and the size of gel beads are the main
263 factors affecting the Ca^{2+} diffusion into alginate gel beads during gelation. It has been
264 reported that higher alginate concentrations incorporated more calcium ions in alginate gel
265 beads (Quong, et al., 1998). In this study, all gel beads were prepared with 2% (w/w)
266 $\text{CaCl}_2 \cdot 2\text{H}_2\text{O}$ solutions, and the size of samples 1A ($r_{\max} = 2.1$ mm and $r_{\min} = 2.0$ mm), 1A1S

267 ($r_{\max} = 2.2$ and $r_{\min} = 2.1$), and 1A1S20O ($r_{\max} = 2.1$ and $r_{\min} = 2.0$) did not significantly differ
268 at the end the maturation step. Therefore, it was assumed that the changes in Young's
269 modulus of samples 1A, 1A1S, and 1A1S20O during the maturation step showed a similar
270 trend probably because oil and SPI had no significant effect on the Ca^{2+} diffusion from the
271 CaCl_2 solutions in alginate gel beads during the maturation step.

272 After the maturation step, the Young's modulus of samples 1A and 1A1S decreased before
273 reaching a constant value (Fig. 2A). The concentrations of Ca^{2+} and alginate in alginate gel
274 beads decreases from the gel surface to gel core (Quong, et al., 1998), which indicates that
275 the gel structure of the outer regions of beads is stronger than that of inside gel beads.
276 Therefore, the fragile core structure of gel beads can not support the whole structure, which
277 leads to the collapse of the inner structure at the end of the maturation step and thus a
278 decreased Young's modulus (Puguan, et al., 2014). However, the Young's modulus of
279 sample 1A1S20O reached the balance directly after the maturation step during gelation (Fig.
280 2A). This was probably because the structures of sample 1A1S20O are totally different from
281 that of samples 1A and 1A1S. After introducing oil into 1A1S dispersions, oil droplets
282 disperse in the alginate solutions during homogenization, and SPI molecules move to the
283 surface of oil droplets from the water phase, due to their emulsifying capacity. The resulting
284 emulsions can turn into emulsion gels after alginate monomers are crosslinked by calcium
285 cations, and shrinkage also occurs during this process. However, oil droplets may act as
286 fillers and help to support the structure of gel beads from collapse after the maturation step
287 during gelation. It has also been indicated that the oil core could support the shell of silica
288 gels from fracture during the sol-gel process (Liang, Liu, Zhang, Qu, Li, & Yang, 2011).
289 Therefore, it was also assumed that oil played an important role on preventing the structural
290 collapse of alginate gel beads during gelation.

291 The effect of concentrations of alginate (Fig. 2B), SPI (Fig. 2C) and sunflower oil (Fig. 2D)
292 on the profiles of Young's modulus of emulsion gel beads during gelation was further
293 investigated. Fig. 2B shows that the Young's modulus of sample 0.5A1S20O increased
294 initially, decreased between 4 and 8 min, and then increased again, before reaching a plateau.
295 In this sample, the structure of gel matrix formed by 0.5% alginate is fragile during the
296 maturation step, which results in severe structural collapse before compact emulsion droplets
297 can support emulsion gel structures. However, samples 1A1S20O and 1.5A1S20O showed a
298 similar trend, in which the Young's modulus increased up to 8 min and then reached a
299 plateau (Fig. 2B). This indicates that increasing alginate concentrations from 0.5% to 1.5%
300 not only slowed Ca^{2+} diffusion and thus caused a slowing of the maturation step but also
301 formed stronger alginate-based matrix structures and thus protected emulsion gel structures
302 from collapse during gelation. Figs. 2C and 2D show that increasing SPI concentrations from
303 0.5% to 2.0% and oil contents from 10% to 40% had no significant effect on the profiles of
304 Young's modulus during gelation (i.e., reaching the plateau directly after the maturation step
305 at around 8 min during gelation). This was probably because increasing concentrations of SPI
306 and oil had no significant impact on calcium diffusion in emulsion gel beads, and 10% oil
307 was high enough to prevent structural collapse of emulsion gel beads after the maturation step
308 during gelation.

309 3.2.2. Effect of alginate, SPI and oil on the Young's modulus of gel beads after gelation

310 Mechanical properties are important for emulsion gels because they are closely associated
311 with other properties (e.g., storage stability, oral perception, and controlled release of
312 encapsulated nutrients). Many factors can affect mechanical properties of emulsion gels, such
313 as gel strength of gel matrix structures (i.e., protein and polysaccharide), modulus of filler
314 droplets, and interactions between oil droplets and the gel matrix. Therefore, the effect of
315 concentrations of alginate, oil and SPI on the Young's modulus of emulsion gel beads was

316 investigated in this study, and all samples were compared after they were allowed to gel for
317 30 min in CaCl₂ solutions (Figs. 2B–D).

318 Fig. 2B shows that increasing alginate concentrations from 0.5 to 1.5% significantly
319 increased the Young's modulus of emulsion gel beads. This was expected because increasing
320 alginate concentration could increase gel strength of alginate-based gel matrix and thus
321 increase the Young's modulus of overall emulsion gels. Similarly, it has previously been
322 reported that increasing agar content (from 1.0 to 1.8%) in o/w emulsions containing 0.1
323 volume fraction of corn oil decreased the overall volume of void spaces and increased strand
324 compactness of emulsion gels (Kim, Gohtani, Matsuno, & Yamano, 1999).

325 Fig. 2D indicates that increasing oil contents from 10% to 40% had no significant effect on
326 the Young's modulus of emulsion gel beads. According to the interactions between
327 emulsifier-coated emulsion droplets and the gel matrix, oil droplets can be divided into active
328 and inactive fillers (also known as bound and unbound fillers) in emulsion gels (Dickinson,
329 2012; Yang et al., 2020). Active fillers are mechanically connected to the gel network by
330 noncovalent and/or covalent bonds through emulsifiers. For examples, it has been reported
331 that WPI-coated oil droplets could be bound to a WPI-based gel matrix by covalent
332 interactions (e.g., hydrophobic interactions and sulphur bridges) (Sala, de Wijk, van de
333 Velde, and van Aken, 2008); it has been also indicated that lactoferrin-stabilised emulsion
334 droplets could bind to a κ -carrageenan gel, probably because of electrostatic interactions
335 between positively charged lactoferrin (pI = 8.2) and negatively charged κ -carrageenan at pH
336 7–8 (Sala, van Vliet, Cohen Stuart, Aken, and van de Velde, 2009). In addition, the Kerner
337 model can explain the effect of active fillers on the mechanical properties of emulsion gels
338 (Kerner, 1956). According to this model, increasing the volume fraction (ϕ_f) of active fillers
339 can increase the mechanical properties of emulsion gels, which has been supported by many
340 studies (Oliver, Berndsen, van Aken, & S  holten, 2015; Sala, et al., 2009). However, in this

341 study, SPI ($pI = 4.5$) and alginate were both negatively charged at pH 6.5–7.0, so there are no
342 electrostatic interactions between SPI-coated droplets and alginate-based gel matrix. It is also
343 unlikely that SPI-coated droplets can connect to the alginate-based gel network by covalent
344 interactions. Additionally, the results obtained in this study were in a disaccord with the
345 Kerner model. Therefore, it was assumed that SPI-coated droplets were inactive fillers in
346 alginate-based emulsion gel beads.

347 Fig. 2C shows that increasing SPI concentrations decreased the Young's modulus of
348 emulsion gel beads. According to the state of emulsion droplets in gels, structures of
349 emulsion gels can be divided into two categories: emulsion droplet-filled gels and emulsion
350 droplet-aggregated gels (Dickinson, 2012). In emulsion droplet-filled gels, the continuous
351 phase (e.g., protein- and polysaccharide-based gels) forms a continuous gel matrix, and
352 emulsion droplets are embedded in this gel matrix. In emulsion droplet-aggregated gels,
353 emulsion droplets aggregate together and form a network structure, such that the gel matrix is
354 disrupted by the aggregated emulsion droplets. As shown in Figs. 1B and 1D, more
355 aggregations of emulsion droplets occurred in sample 1A2S20O compared to sample
356 1A1S20O, probably because increasing SPI concentration led to more depletion flocculation
357 of SPI-coated droplets in emulsions (Lam & Nickerson, 2013). In active droplet-aggregated
358 gels, the crowding effect of fillers (particle interactions) increases the shear modulus of the
359 overall gels (Oliver, et al., 2015). However, SPI-coated droplets in alginate-based gel matrix
360 may act as inactive fillers as discussed before in this study. Therefore, it was assumed that
361 increased aggregation of SPI-coated droplets (inactive fillers) had a negative effect on the
362 Young's modulus of alginate-based emulsion gel beads, probably because aggregated
363 droplets (i.e., the increased phase separation between alginate-based gel matrix and SPI-
364 coated droplets) may disturb the formation of alginate-based network structures (Dickinson,
365 2012; Lin, Lu, Kelly, Zhang, Zheng, & Miao, 2017).

366 *3.3 Water loss of gel beads*

367 During the maturation step, inter-chain interactions between stretches of alginate monomers
368 and Ca^{2+} occurred with the diffusion of Ca^{2+} from the surface to interior of gel beads, and the
369 formation of junctions between these stretches forced water out, which led to shrinkage and
370 increased water loss of gel beads during gelation (Puguan, et al., 2014; Rehm, 2009). Fig. 3
371 shows the effects of concentrations of alginate, SPI, and oil on the water loss from emulsion
372 gel beads during gelation. It indicates that increasing alginate contents (from 0.5 to 1.5%) or
373 SPI concentration (from 0.5 to 2.0%) had no significant effect on the rates of water loss, but
374 increasing oil content (from 10 to 40%) could slow the water loss in terms of the profiles of
375 water loss during gelation, probably because lower water content of the original emulsions
376 results in slower water loss of emulsion gels during gelation.

377 Fig. 3 also indicates that the water loss of emulsion gel beads after gelation for 30 min
378 decreased with increasing alginate contents (from 0.5 to 1.5%), SPI concentration (from 0.5
379 to 2.0%) and oil content (from 10 to 40%). Many factors can affect the water loss of emulsion
380 gel beads during gelation, such as the concentration of CaCl_2 solutions, the water content of
381 original emulsions, the strength of gel matrix, and the hydrophilicity and rigidity of fillers. It
382 has been reported that increasing the concentration of CaCl_2 solution (from 0.08 M to 0.3 M)
383 reduced the final weight of alginate gel beads due to the increased water loss (Puguan, et al.,
384 2014), but in this study all samples were dropped into the CaCl_2 solutions with the same
385 concentration. Therefore, increasing alginate concentration from 0.5% to 1.5% decreased the
386 water loss of beads from $42.3 \pm 1.2\%$ to $36.9 \pm 0.3\%$ after gelation (Fig. 3A), which was
387 probably because elastic modulus of gel beads increased with increasing alginate
388 concentration (Fig. 2B), and gels with stronger matrix structures had better water-binding
389 capacity.

390 In addition, increasing SPI concentration from 0.5% to 2.0% decreased the water loss of
391 emulsion gel beads from $40.2 \pm 0.6\%$ to $37.3 \pm 0.3\%$ after gelation as well (Figs. 3B),
392 probably due to increased water-absorption capacity of SPI-coated droplets. Denatured SPI
393 has emulsifying capacity because it has both hydrophobic and hydrophilic groups (Nishinari,
394 et al., 2014). As shown in Figs. 1A and 1B, SPI aggregated in sample 1A1S but formed a film
395 at the oil-water interface in sample 1A1S20O, in which hydrophobic groups of SPI connected
396 to oil droplets and hydrophilic groups connected to water. Therefore, more SPI was absorbed
397 at the surface of emulsion droplets by increasing SPI concentration (Fig. 1D), which resulted
398 in increased hydrophilicity of SPI-coated droplets and increased water-retention capacity of
399 emulsion gel beads (Wang, Marcone, Barbut, & Lim, 2012). This explanation could be
400 supported by previous conclusions by Wagner, et al. (1990) that SPI with highly denatured
401 proteins and high surface hydrophobicity exhibited the highest water-absorption capacity.
402 Additionally, increasing oil content from 10% to 40% led to the decreased water loss of
403 emulsion gel beads (from $46.1 \pm 0.2\%$ to $25.1 \pm 0.4\%$ after gelation) (Figs. 3C), probably
404 because the water content in original emulsions significantly decreased with increasing oil
405 contents from 10% to 40%, and emulsion droplets could protect gel structures from collapse
406 as well. A similar finding has been reported where increasing the oil volume fraction (13%–
407 31.1%) in β -lactoglobulin-based oil-in-water emulsions improved the water-retention
408 capacity of emulsion gels (Line, Remondetto, & Subirade, 2005).

409 *3.4 Morphological properties and shrinkage of gel beads*

410 As shown in Fig. 4, alginate gel beads (1A) were transparent, but the presence of SPI
411 decreased the transparency of alginate gel beads (1A1S) because of its yellow colour, and
412 introducing oil led to ivory gel beads, due to the formation of emulsions. In addition, gel
413 beads in all groups were not completely spherical, and samples 1.5A1s20O, 1A2S20O, and
414 1A1S40O had small tails. This was because increasing the concentrations of alginate, SPI and

415 oil could raise the viscosity of emulsions (Fig. 5), which could affect the morphological
416 properties of emulsion gel beads. In this study, we used the simple dripping method to
417 produce emulsion gel beads. The emulsions were pushed out from pipette and one droplet
418 was formed at the tip before the droplet grew in size gradually and dropped into CaCl_2
419 solutions. During this process, spherical emulsion droplets were formed because of the
420 surface tension of liquid (Ching, et al., 2017). However, Lević, et al. (2015) found that D-
421 limonene could increase the viscosity and reduce the conductivity of the alginate liquid
422 systems by changing structural ordering of alginate, which indicates that the high viscosity of
423 emulsion was against the formation of spherical bead at the tip of pipet because of poor flow
424 properties. For example, the introduction of hydroxypropylmethylcellulose (0.2%–1%)
425 changed the rheological properties of 2% alginate solutions and produced beads with small
426 tails (Bellich, Borgogna, Cok, and Cesàro, 2011).

427 Fig. 4 also shows that the size of all samples decreased during gelation and, in order to
428 compare their shrinkage during gelation, the section shrinkage rates were calculated (Fig. 6).
429 The profiles of shrinkage rates show that shrinkage rates of all samples increased during
430 gelation, probably due to syneresis (i.e., water loss) and structural collapse (Rehm, 2009).
431 However, in terms of the profiles of shrinkage rate, increasing contents of alginate and oil
432 could slow the shrinkage, but increasing SPI content had no significant effect on the rate of
433 shrinkage during gelation. Fig.6 also shows that the shrinkage rates decreased from $26.7 \pm$
434 2.1% to $18.2 \pm 2.2\%$ and from $27.1 \pm 1.6\%$ to $13.6 \pm 2.5\%$ after gelation with increasing
435 concentrations of alginate (from 0.5% to 1.5%) and oil (from 10% to 40%), respectively, but
436 increasing SPI concentration from 0.5% to 2.0% had no significant effect on the shrinkage
437 rates of emulsion gel beads after gelation for 30 min. Many factors can affect the shrinkage of
438 emulsion gels during gelation, such as water loss, gel stiffness, the content and properties of
439 fillers, and interactions between fillers and the continuous phase (Smith, Scherer, &

440 Anderson, 1995). In terms of alginate, increasing its concentration could increase the elastic
441 modulus of emulsion gel beads (Fig. 2B), which may provide resistance to shrinkage
442 (Brinker, et al., 1994). Increasing oil concentration led to more compact filler structures,
443 which resisted further shrinkage during gelation as seen on comparing emulsion gel structures
444 of samples 1A1S20O and 1A1S40O in Fig. 1. Eichler, Ramon, Ladyzhinski, Cohen, &
445 Mizrahi (1997) also indicated similar conclusions, in that fructose or polydextrose being
446 introduced into polyacrylamide (PAAm) gels could act as a mechanical barrier against further
447 volume shrinkage of PAAm gels during dehydration. However, increasing SPI concentration
448 reduced the Young's modulus (Fig. 2C) but increased water retention (i.e., decreased water
449 loss) (Fig. 3B) of emulsion gel beads, which may explain why increasing SPI concentration
450 had no significant effects on shrinkage rates of emulsion gel beads.

451 **4. Conclusions**

452 The Young's modulus of alginate-based emulsion gel beads kept increasing before reaching a
453 plateau during gelation process. This gelation process was accompanied by syneresis (i.e.,
454 water loss) and shrinkage, which resulted in an increased compactness of emulsion gel beads.
455 SPI-coated droplets could maintain their structures during gelation. With increasing alginate
456 concentration (0.5%–1.5%), the water loss decreased, the Young's modulus increased, and
457 shrinkage rate decreased. Increasing SPI concentration (0.5%–2.0%) led to decreased
458 Young's modulus and water loss, and undifferentiated shrinkage. Higher oil content (10%–
459 40%) decreased water loss and section shrinkage rates, and had no significant effect on the
460 Young's modulus. These findings underlined the effect of concentrations of components on
461 the properties of emulsion gel beads during gelation, which are very important because the
462 properties of emulsion gel beads may affect encapsulation, stability, and release of
463 hydrophobic functional ingredients encapsulated in emulsion gel beads.

464 **Acknowledgement**

465 This work is supported by the China Scholarship Council (No. 201708350111) and Teagasc-
466 The Irish Agriculture and Food Development Authority (RMIS6821). The assistance of
467 Helen Slattery with the freeze-drying system and Deirdre Kennedy with confocal scanning
468 laser microscopy is highly appreciated.

469 **References**

- 470 Bellich, B., Borgogna, M., Cok, M., & Cesàro, A. (2011). Release properties of hydrogels: Water
471 evaporation from alginate gel beads. *Food Biophysics*, *6*, 259-266.
- 472 Brinker, C. J., Sehgal, R., Hietala, S., Deshpande, R., Smith, D., Loy, D., & Ashley, C. (1994). Sol-
473 gel strategies for controlled porosity inorganic materials. *Journal of Membrane Science*, *94*,
474 85-102.
- 475 Brito-Oliveira, T. C., Bispo, M., Moraes, I. C. F., Campanella, O. H., & Pinho, S. C. (2017). Stability
476 of curcumin encapsulated in solid lipid microparticles incorporated in cold-set emulsion filled
477 gels of soy protein isolate and xanthan gum. *Food Research International*, *102*, 759-767.
- 478 Ching, S. H., Bansal, N., & Bhandari, B. (2016). Rheology of emulsion-filled alginate microgel
479 suspensions. *Food Research International*, *80*, 50-60.
- 480 Ching, S. H., Bansal, N., & Bhandari, B. (2017). Alginate gel particles—A review of production
481 techniques and physical properties. *Critical Reviews in Food Science & Nutrition*, *57*, 1133-
482 1152.
- 483 Corstens, M. N., Berton-Carabin, C. C., Elichiry-Ortiz, P. T., Hol, K., Troost, F. J., Masclee, A. A.
484 M., & Schroën, K. (2017). Emulsion-alginate beads designed to control in vitro intestinal
485 lipolysis: Towards appetite control. *Journal of Functional Foods*, *34*, 319-328.
- 486 Dickinson, E. (2012). Emulsion gels: The structuring of soft solids with protein-stabilized oil droplets.
487 *Food Hydrocolloids*, *28*, 224-241.
- 488 Eichler, S., Ramon, O., Ladyzhinski, I., Cohen, Y., & Mizrahi, S. (1997). Collapse processes in
489 shrinkage of hydrophilic gels during dehydration. *Food Research International*, *30*, 719-726.

- 490 Geremias-Andrade, I. M., Souki, N. P. D. B. G., Moraes, I. C. F., & Pinho, S. C. (2017). Rheological
491 and mechanical characterization of curcumin-loaded emulsion-filled gels produced with whey
492 protein isolate and xanthan gum. *LWT - Food Science and Technology*, *86*, 166-173.
- 493 Guo, Q., Bellissimo, N., & Rousseau, D. (2017). Role of gel structure in controlling in vitro intestinal
494 lipid digestion in whey protein emulsion gels. *Food Hydrocolloids*, *69*, 264-272.
- 495 Kerner, E. (1956). The elastic and thermo-elastic properties of composite media. *Proceedings of the*
496 *Physical Society. Section B*, *69*, 808.
- 497 Kim, K., Gohtani, S., Matsuno, R., & Yamano, Y. (1999). Effects of oil droplet and agar
498 concentration on gel strength and microstructure of o-w emulsion gel. *Journal of Texture*
499 *Studies*, *30*, 319-335.
- 500 King, A. (1983). Brown seaweed extracts (alginates). *Food Hydrocolloids*, *2*, 115-188.
- 501 Lam, R. S., & Nickerson, M. T. (2013). Food proteins: A review on their emulsifying properties using
502 a structure-function approach. *Food Chemistry*, *141*, 975-984.
- 503 Lević, S., Pajić Lijaković, I., Đorđević, V., Rac, V., Rakić, V., Šolević Knudsen, T., Pavlović, V.,
504 Bugarski, B., & Nedović, V. (2015). Characterization of sodium alginate/D-limonene
505 emulsions and respective calcium alginate/D-limonene beads produced by electrostatic
506 extrusion. *Food Hydrocolloids*, *45*, 111-123.
- 507 Liang, F., Liu, J., Zhang, C., Qu, X., Li, J., & Yang, Z. (2011). Janus hollow spheres by emulsion
508 interfacial self-assembled sol-gel process. *Chemical Communications*, *47*, 1231-1233.
- 509 Lin, D., Lu, W., Kelly, A. L., Zhang, L., Zheng, B., & Miao, S. (2017). Interactions of vegetable
510 proteins with other polymers: Structure-function relationships and applications in the food
511 industry. *Trends in Food Science & Technology*, *68*, 130-144.
- 512 Line, V. L.S., Remondetto, G. E., & Subirade, M. (2005). Cold gelation of β -lactoglobulin oil-in-
513 water emulsions. *Food Hydrocolloids*, *19*, 269-278.
- 514 Ma, D., Tu, Z.-C., Wang, H., Zhang, Z., & McClements, D. J. (2017). Fabrication and
515 characterization of nanoemulsion-coated microgels: Electrostatic deposition of lipid droplets
516 on alginate beads. *Food Hydrocolloids*, *71*, 149-157.

- 517 Ma, L., Wan, Z., & Yang, X. (2017). Multiple water-in-oil-in-water emulsion gels based on self-
518 assembled saponin fibrillar network for photosensitive cargo protection. *Journal of*
519 *Agricultural and Food Chemistry*, 65, 9735-9743.
- 520 Moschakis, T., Murray, B. S., & Biliaderis, C. G. (2010). Modifications in stability and structure of
521 whey protein-coated o/w emulsions by interacting chitosan and gum arabic mixed
522 dispersions. *Food hydrocolloids*, 24, 8-17.
- 523 Natrajan, D., Srinivasan, S., Sundar, K., & Ravindran, A. (2015). Formulation of essential oil-loaded
524 chitosan-alginate nanocapsules. *Journal of Food and Drug Analysis*, 23, 560-568.
- 525 Nishinari, K., Fang, Y., Guo, S., & Phillips, G. O. (2014). Soy proteins: A review on composition,
526 aggregation and emulsification. *Food Hydrocolloids*, 39, 301-318.
- 527 Oliver, L., Berndsen, L., van Aken, G. A., & Scholten, E. (2015). Influence of droplet clustering on
528 the rheological properties of emulsion-filled gels. *Food Hydrocolloids*, 50, 74–83.
- 529 Pintado, T., Ruiz-Capillas, C., Jimenez-Colmenero, F., Carmona, P., & Herrero, A. M. (2015). Oil-in-
530 water emulsion gels stabilized with chia (*Salvia hispanica L.*) and cold gelling agents:
531 Technological and infrared spectroscopic characterization. *Food Chemistry*, 185, 470–478.
- 532 Piornos, J. A., Burgos-Díaz, C., Morales, E., Rubilar, M., & Acevedo, F. (2017). Highly efficient
533 encapsulation of linseed oil into alginate/lupin protein beads: Optimization of the emulsion
534 formulation. *Food Hydrocolloids*, 63, 139-148.
- 535 Puguán, J. M., Yu, X., & Kim, H. (2014). Characterization of structure, physico-chemical properties
536 and diffusion behavior of Ca-Alginate gel beads prepared by different gelation methods.
537 *Journal of Colloid and Interface Science*, 432, 109-116.
- 538 Quong, D., Neufeld, R., Skjåk-Bræk, G., & Poncelet, D. (1998). External versus internal source of
539 calcium during the gelation of alginate beads for DNA encapsulation. *Biotechnology and*
540 *Bioengineering*, 57, 438-446.
- 541 Rehm, B. H. A. (Ed.). (2009). *Alginates: biology and applications*. Heidelberg: Springer.
- 542 Rosa, P., Sala, G., Van Vliet, T., & Van De Velde, F. (2006). Cold gelation of whey protein
543 emulsions. *Journal of Texture Studies*, 37, 516-537.

- 544 Sala, G., de Wijk, R. A., van de Velde, F., & van Aken, G. A. (2008). Matrix properties affect the
545 sensory perception of emulsion-filled gels. *Food Hydrocolloids*, 22, 353-363.
- 546 Sala, G., van Vliet, T., Cohen Stuart, M. A., Aken, G. A. v., & van de Velde, F. (2009). Deformation
547 and fracture of emulsion-filled gels: Effect of oil content and deformation speed. *Food*
548 *Hydrocolloids*, 23, 1381–1393.
- 549 Sato, A. C. K., Moraes, K. E. F. P., & Cunha, R. L. (2014). Development of gelled emulsions with
550 improved oxidative and pH stability. *Food Hydrocolloids*, 34, 184–192.
- 551 Smith, D., Scherer, G., & Anderson, J. (1995). Shrinkage during drying of silica gel. *Journal of Non-*
552 *Crystalline Solids*, 188, 191-206.
- 553 Tavernier, I., Patel, A. R., Van der Meeren, P., & Dewettinck, K. (2017). Emulsion-templated liquid
554 oil structuring with soy protein and soy protein: κ -carrageenan complexes. *Food*
555 *Hydrocolloids*, 65, 107-120.
- 556 Urbonaite, V., de Jongh, H. H. J., van der Linden, E., & Pouvreau, L. (2015). Water holding of soy
557 protein gels is set by coarseness, modulated by calcium binding, rather than gel stiffness.
558 *Food Hydrocolloids*, 46, 103-111.
- 559 Van Vliet, T. (1988). Rheological properties of filled gels: Influence of filler matrix interaction.
560 *Colloid and Polymer Science*, 266, 518-524.
- 561 Vasile, F. E., Judis, M. A., & Mazzobre, M. F. (2018). Impact of Prosopis alba exudate gum on
562 sorption properties and physical stability of fish oil alginate beads prepared by ionic gelation.
563 *Food Chemistry*, 250, 75-82.
- 564 Wagner, J., & Añón, M. C. (1990). Influence of denaturation, hydrophobicity and sulfhydryl content
565 on solubility and water absorbing capacity of soy protein isolates. *Journal of Food Science*,
566 55, 765-770.
- 567 Wang, S., Marcone, M., Barbut, S., & Lim, L. T. (2012). The impact of anthocyanin-rich red
568 raspberry extract (ARRE) on the properties of edible soy protein isolate (SPI) films. *Journal*
569 *of Food Science*, 77, C497-505.

- 570 Wang, Z., Neves, M. A., Kobayashi, I., Uemura, K., & Nakajima, M. (2013). Preparation,
571 characterization, and in vitro gastrointestinal digestibility of oil-in-water emulsion-agar gels.
572 *Bioscience Biotechnology and Biochemistry*, 77, 467-474.
- 573 Yang, N., Feng, Y. N., Su, C. X., Wang, Q., Zhang, Y. M., Wei, Y. H., Zhao, M., Nishinari, K., Fang,
574 Y. P. (2020). Structure and tribology of κ -carrageenan gels filled with natural oil bodies. *Food*
575 *hydrocolloids*, 105945.
- 576 Yin, L., Zhao, Z., Hu, Y., Ding, J., Cui, F., Tang, C., & Yin, C. (2008). Polymer-protein interaction,
577 water retention, and biocompatibility of a stimuli-sensitive superporous hydrogel containing
578 interpenetrating polymer networks. *Journal of Applied Polymer Science*, 108, 1238-1248.
- 579 Zhang, Z. P., Zhang, R. J., Zou, L. Q., Chen, L., Ahmed, Y., Bishri, W. A., Balamash, K., &
580 McClements, D. J. (2016). Encapsulation of curcumin in polysaccharide-based hydrogel
581 beads. *Food Hydrocolloids*, 58, 160-170.
- 582

583 **Table 1**

584 Formulations of experimental emulsions.

Group	Water phase ^a		Oil Con. (% wt)
	Alginate Con. (% wt)	Soy protein Con. (% wt)	
1A (Control 1)	1.0	0	0
1A1S (Control 2)	1.0	1.0	0
1A1S20O	1.0	1.0	20
0.5A1S20O	0.5	1.0	20
1.5A1S20O	1.5	1.0	20
1A0.5S20O	1.0	0.5	20
1A2S20O	1.0	2.0	20
1A1S10O	1.0	1.0	10
1A1S40O	1.0	1.0	40

585 ^aThe content of water phase was adjusted according to the oil content in the formulation.

Figure Legends

Fig. 1. CLSM images of dispersions/emulsions (A–E) and gel beads (V–Z) after gelation for 30 min. SPI and sunflower oil were stained by red and green, respectively.

Fig. 2. Kinetics of Young's modulus of alginate-based gel beads during gelation: (A) control groups; (B) effect of alginate concentrations (0.5–1.5% in the water phase); (C) effect of SPI concentrations (0.5–2.0% in the water phase); and (D) effect of oil contents (10–40% in the emulsion).

Fig. 3. Kinetics of water loss from alginate-based gel beads during gelation: (A) effect of alginate concentrations (0.5–1.5% in the water phase); (B) effect of SPI concentrations (0.5–2.0% in the water phase); and (C) effect of oil contents (10–40% in the emulsion).

Fig. 4. Visual aspects of alginate-based gel beads during gelation (minimum scale mark = 1 mm).

Fig. 5. Viscosity of dispersions/emulsions with different component concentrations.

Fig. 6. Kinetics of section shrinkage of alginate-based gel beads during gelation: (A) effect of alginate concentrations (0.5–1.5% in the water phase); (B) effect of SPI concentrations (0.5–2.0% in the water phase); and (C) effect of oil contents (10–40% in the emulsion).

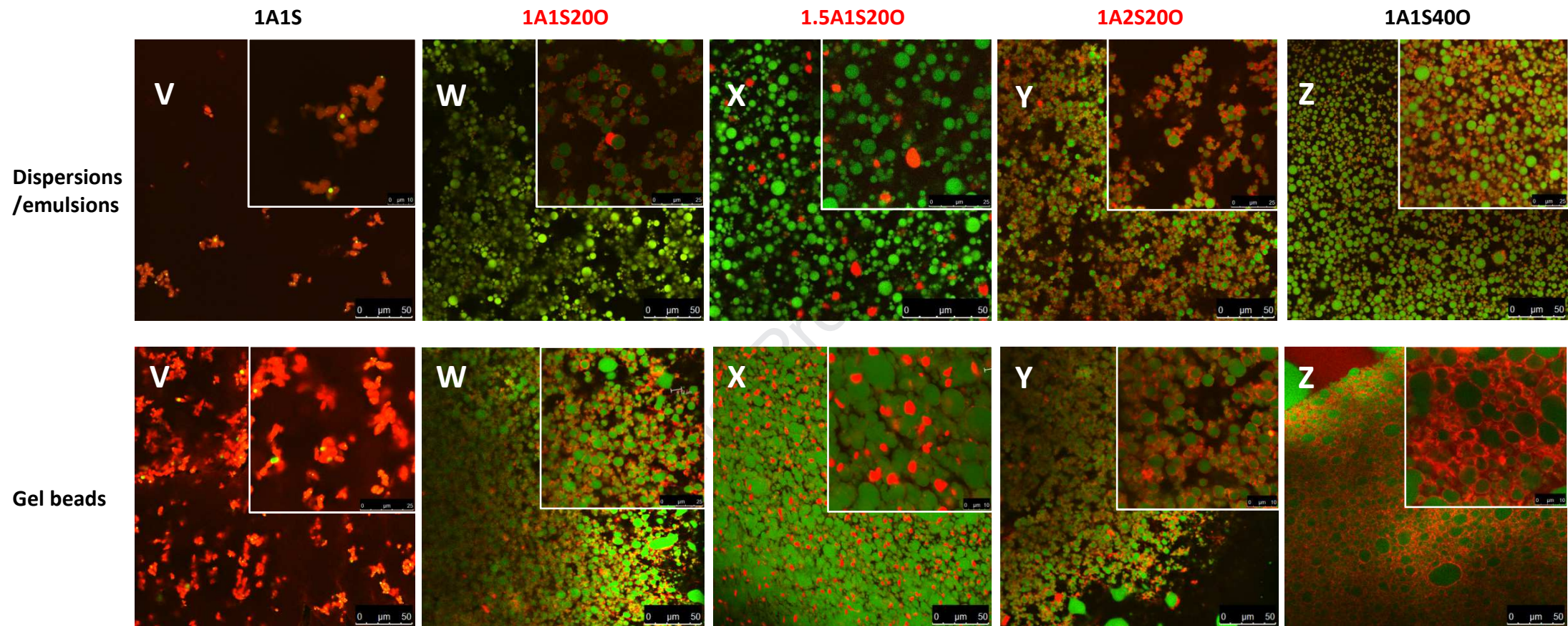


Fig. 1

Journal Pre-proof

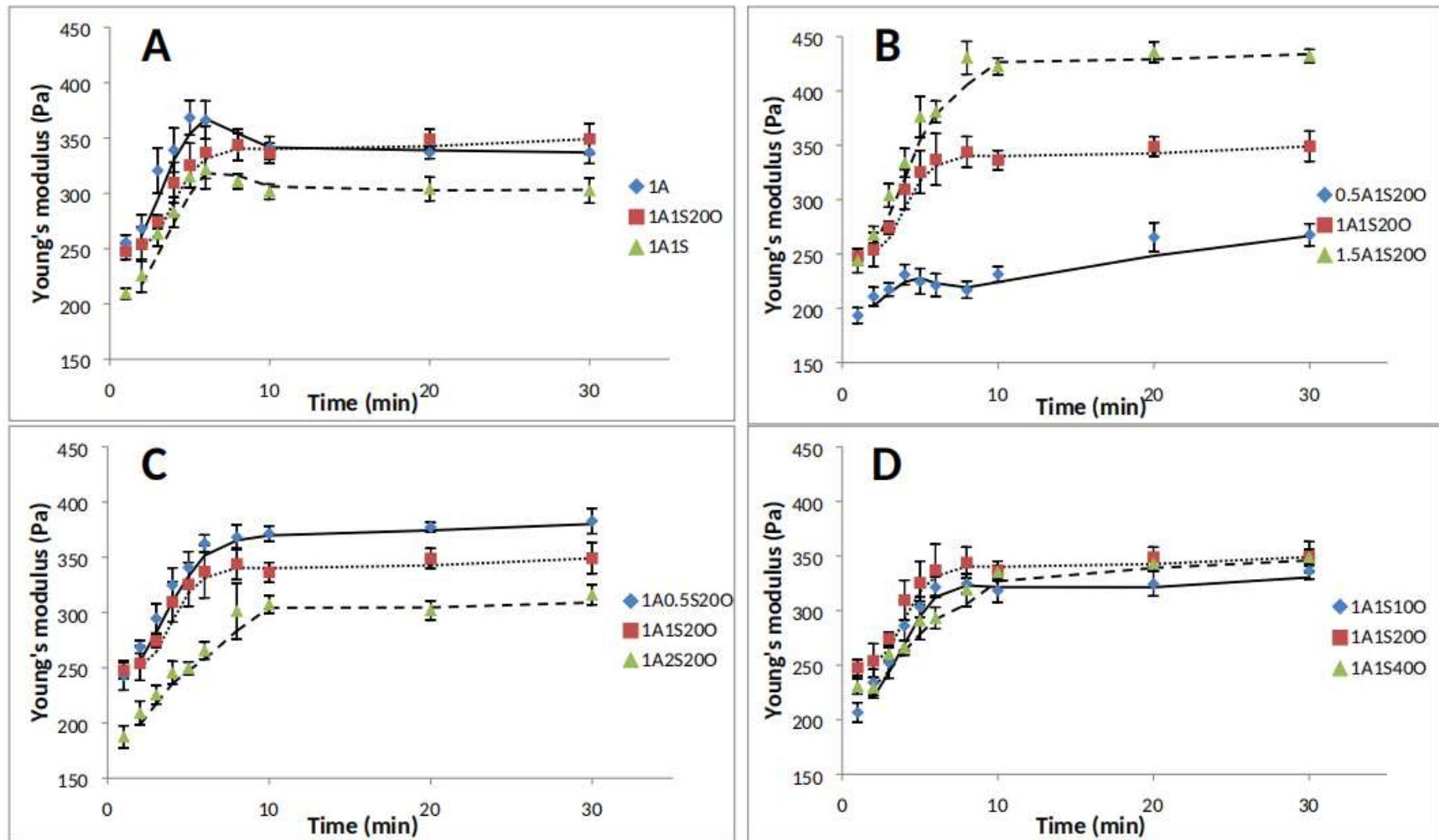


Fig. 2

Journal Pre-proof

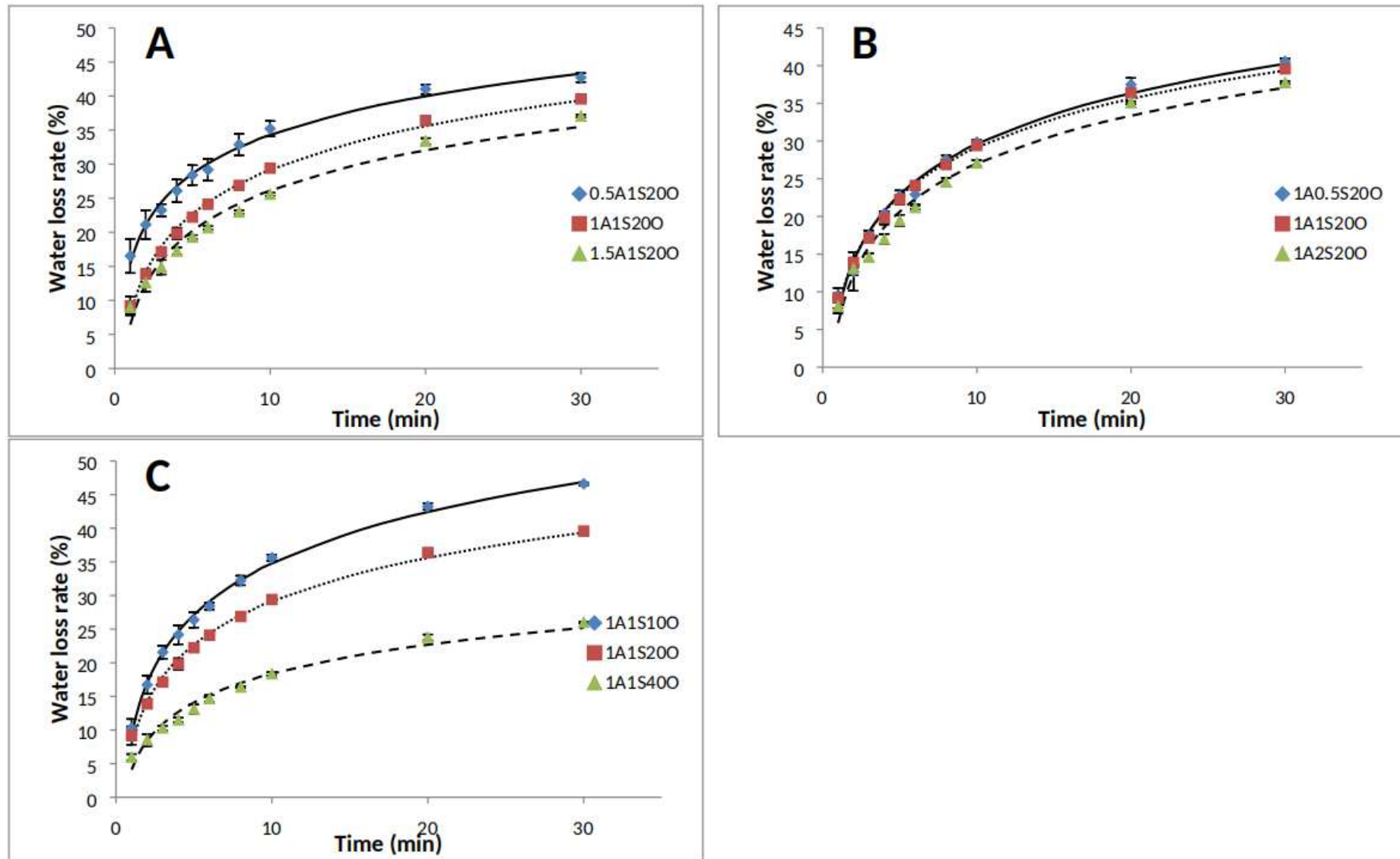


Fig. 3

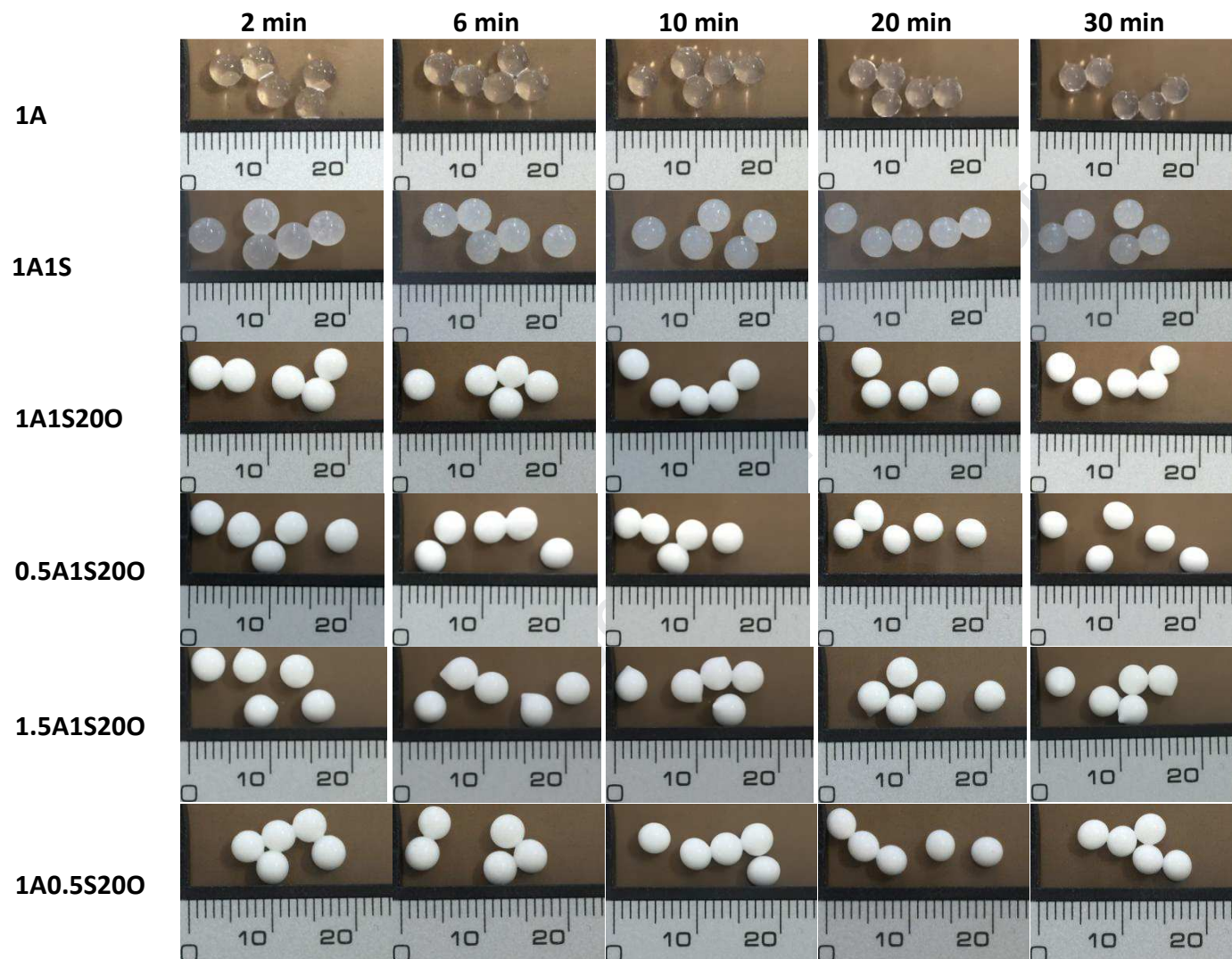




Fig. 4

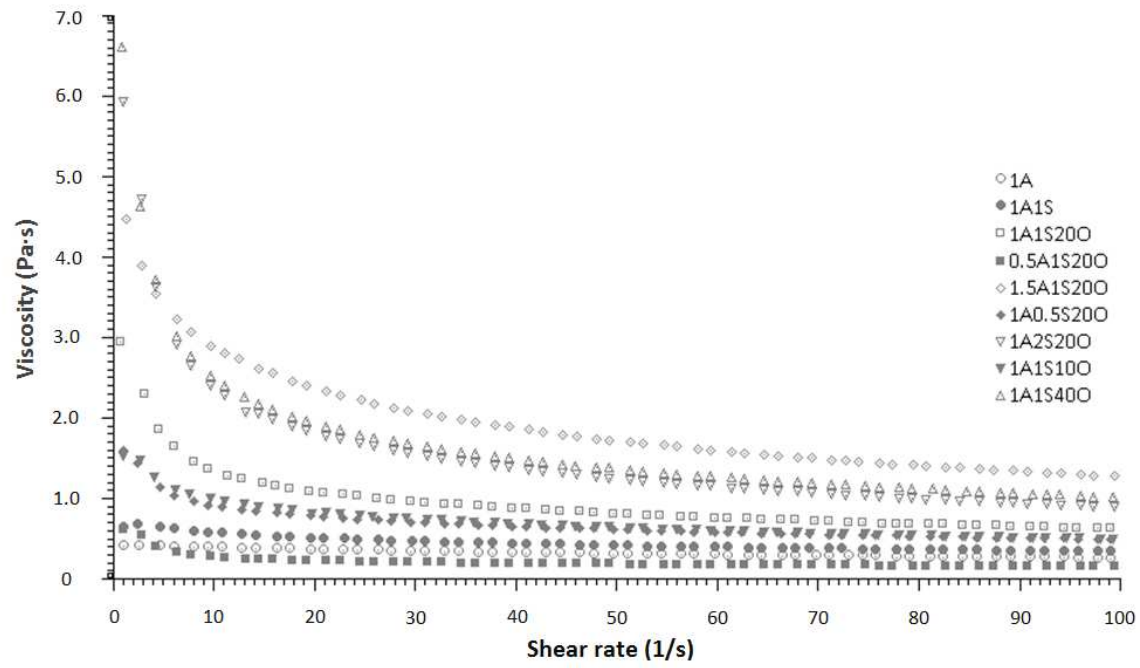


Fig. 5

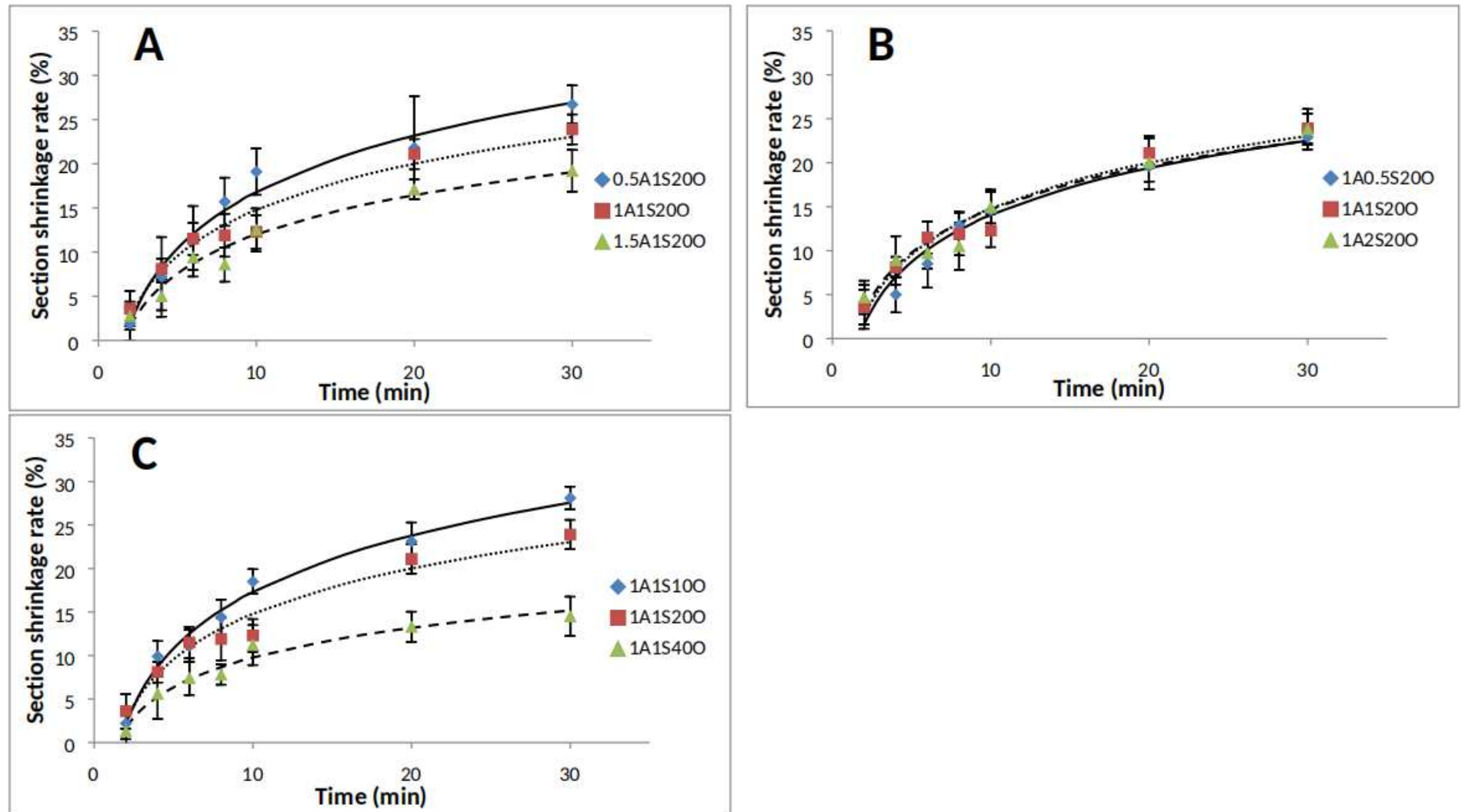


Fig. 6

Highlights

- The Young's modulus of emulsion gel beads increased before reaching a plateau during gelation.
- The gelation of emulsion gel beads was accompanied by syneresis and shrinkage.
- High SPI and oil content led to re-coalescence of emulsion droplets during gelation.
- Increasing SPI content decreased the Young's modulus of emulsion gel beads.
- Increasing oil content decreased the shrinkage of emulsion gel beads.

Duanquan Lin: Conceptualization, Methodology, Writing - original draft, Data curation, investigation.

Alan Kelly: Supervision, writing - review & editing.

Valentyn Maidannyk: Investigation.

Song Miao: Supervision, Conceptualization, Writing - review & editing, Funding acquisition, Project administration, Investigation.

Journal Pre-proof

Declaration of interests

The authors declare that they have no known competing financial interests or personal relationships that could have appeared to influence the work reported in this paper.

The authors declare the following financial interests/personal relationships which may be considered as potential competing interests:

Song Miao

Teagasc Food Research Centre, Moorepark

Journal Pre-proof